Formation of β-C_3N_4 Nanocrystals in Ti-Doped Carbon Nitride Films Prepared by Cathode Arc-Assisted Middle-Frequency Magnetron Sputtering

Zhihong Huang

Wenzhou Polytechnic, Wenzhou 325035, China.

Abstract

Ti-doped carbon nitride thin films have been deposited by cosputtering Ti and graphite targets in a mixed plasma of Ar and N. Transmission electron microscopy revealed that the nucleation of β-C_3N_4 could be promoted by Ti incorporation. The N content of the films was found to strongly depend on Ti concentration, even a small amount of Ti incorporation resulted in a drastic increase in N content. An evolution from amorphous layers with fine mixtures of C, N, and Ti to matrices embedded with β-C_3N_4 nanocrystals was observed with increasing bias voltage.

Keywords

Carbon Nitride, Film, Nanocrystal, TEM, Magnetron Sputter.

1. Introduction

The theoretical work of Liu and Cohen wherein they predicted the hypothetical β-C_3N_4 phase to be harder than diamond has stimulated intense research in carbon nitride (CN_x) materials in recent years [1,2]. Thus far, this material has been synthesized using a variety of technologies, including plasma-assisted chemical vapor deposition [3], ion-beam-assisted deposition [4,5], reactive sputtering [6,7], and laser ablation[8,9]. However, most of the attempts to synthesize this phase have resulted in amorphous graphitic structures. TiN(111) planes have hexagonal symmetry with a unit vector of 3.0 Å. One unit vector (6.44Å) of β-C_3N_4(0001) fits into two unit vectors of TiN(111) with a lattice mismatch of 7%. Thus, TiN was chosen as a structural template for the nucleation of crystalline β-C_3N_4 by Li et al. [10] in their research of CN_x/TiN multiplayer coatings. A high hardness of approximately 45–55 GPa was achieved, but there was insufficient evidence to prove that the formation of β-C_3N_4 crystals occurred. Recently, we have developed an eight-target system that combined cathode arc and middle-frequency magnetron sputtering techniques. In a previous work, Ti-containing amorphous carbon films were prepared by the cosputtering of Ti and graphite, and the enhancement of mechanical properties by nanocrystals was confirmed [11]. In this article, we present a study of Ti-doped CN_x materials produced using this system at various substrate biases, N_2 flow rates, and Ti target currents. Composition and microstructure measurements showed that Ti incorporation facilitated the nucleation of β-C_3N_4 nanocrystals.

2. Experiment

The Ti-doped CN_x films were deposited with the eighttarget cathode arc-assisted middle-frequency closed-field unbalanced magnetron sputter system described in detail elsewhere [11]. Three pairs of graphite targets (purity > 99.99%) and one pair of Ti targets (purity > 99.99%) were mounted vertically in a chamber. P-type Si(111) wafers were used as substrates and placed on a rotating sample carrier with a rotating speed of 5 rev/min. The substrates faced the target at a distance of 100 mm. The base pressure of the chamber was 7×10^{-4} Pa. Before deposition, the substrates were etched in a 2.0 Pa Ar discharge for 30 min, and then were bombarded by Ti ions produced from the Ti cathode arc in Ar ambient at a pressure of 2×10^{-2} Pa for 10 min. The working gases were N_2 and Ar and the working pressure was kept constant at 0.4 Pa. During deposition, the current of the three pairs of C targets was kept constant at 15 A. The deposition time was 2 h. The substrates were not heated and

the chamber ambient temperature was lower than 100ºC. By varying Ti target current, substrate bias, and N_2 flow rate, a batch of samples were prepared. The film thicknesses of all samples are between 600 and 800 nm, as measured using Talysurf Form S4C-3D Profiler. The atomic concentration was determined using an energy dispersive X-ray spectroscopy (EDAX) genesis 7000 EDS system operated at 25 kV. Microstructure studies were carried out by transmission electron microscopy (TEM) JEM-2010FEF (UHR) at 200 kV. TEM specimens were obtained by the standard procedures of precision grinding, dimple grinding, and ion milling until perforation. Raman spectra were measured with a RM-1000 confocal Raman microspectrometer using an Ar ion laser with an excitation wavelength of 514.5 nm.

3. Results and Disscusion

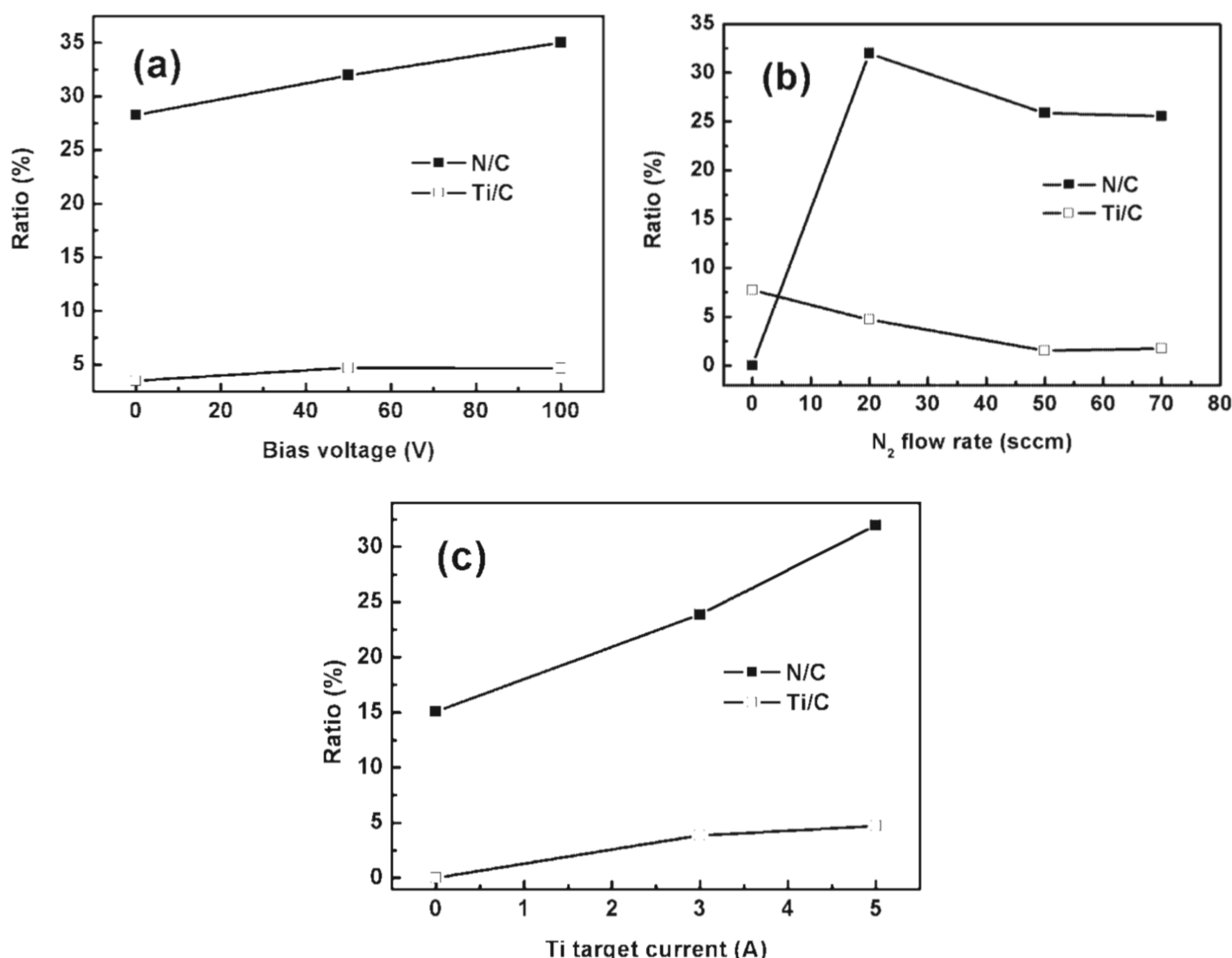

Fig. 1. N/C and Ti/C ratios of CN_x films deposited at various substrate biases (a), N_2 flow rates (b), and Ti target currents (c).

Only Ti, C, N, and a small amount of O were detected in all the films using EDAX. The concentrations of N and Ti relative to C, i.e., N/C and Ti/C, of these samples are shown in Fig. 1. Figure 1(a) shows the effect of bias on Ti and N concentrations. When bias voltage increases from 0 to 100 V, N/C ratio increases from 28 to 35%. This means that more N atoms were incorporated into the films. The increase in bias voltage does not significantly increase Ti concentration. Therefore, an increase in the number of N atoms in the films favored C–N bond formation. Figure 1(b) shows the N/C and Ti/C ratios of the films produced at a fixed bias and target current but at different N_2 flow rates. Ti concentration decreases from 8 to 2% when N_2 flow rate is increased from 0 to 70 sccm. This is a

result of Ti target poisoning. Contrary to conventional nondoped reactive sputtering in which N concentration increases with increasing N_2 partial pressure, N concentration decreases from 32 to 25% with N_2 flow rate increasing from 20 to 70 sccm and exhibits strong dependence on Ti concentration. This dependence is supported by change in N and Ti concentrations with Ti target current, as shown in Fig. 1(c). It can be seen that Ti/C increases from zero when the Ti target is not sputtered to 5% at a Ti target current of 5A, whereas, N/C increases from 15 to 32%. With increasing Ti target current, N/C increases at a rate three times that of Ti/C, which means that the additional N and Ti atoms enter the films with a ratio of approximately 3:1. However, if the incorporation of Ti only formed Ti–N or Ti–C bonds without causing other changes, this ratio would not exceed unity. This means that new structures with high N/C ratio, e.g., N-containing clusters or nanocrystals, are formed as a result of Ti incorporation.

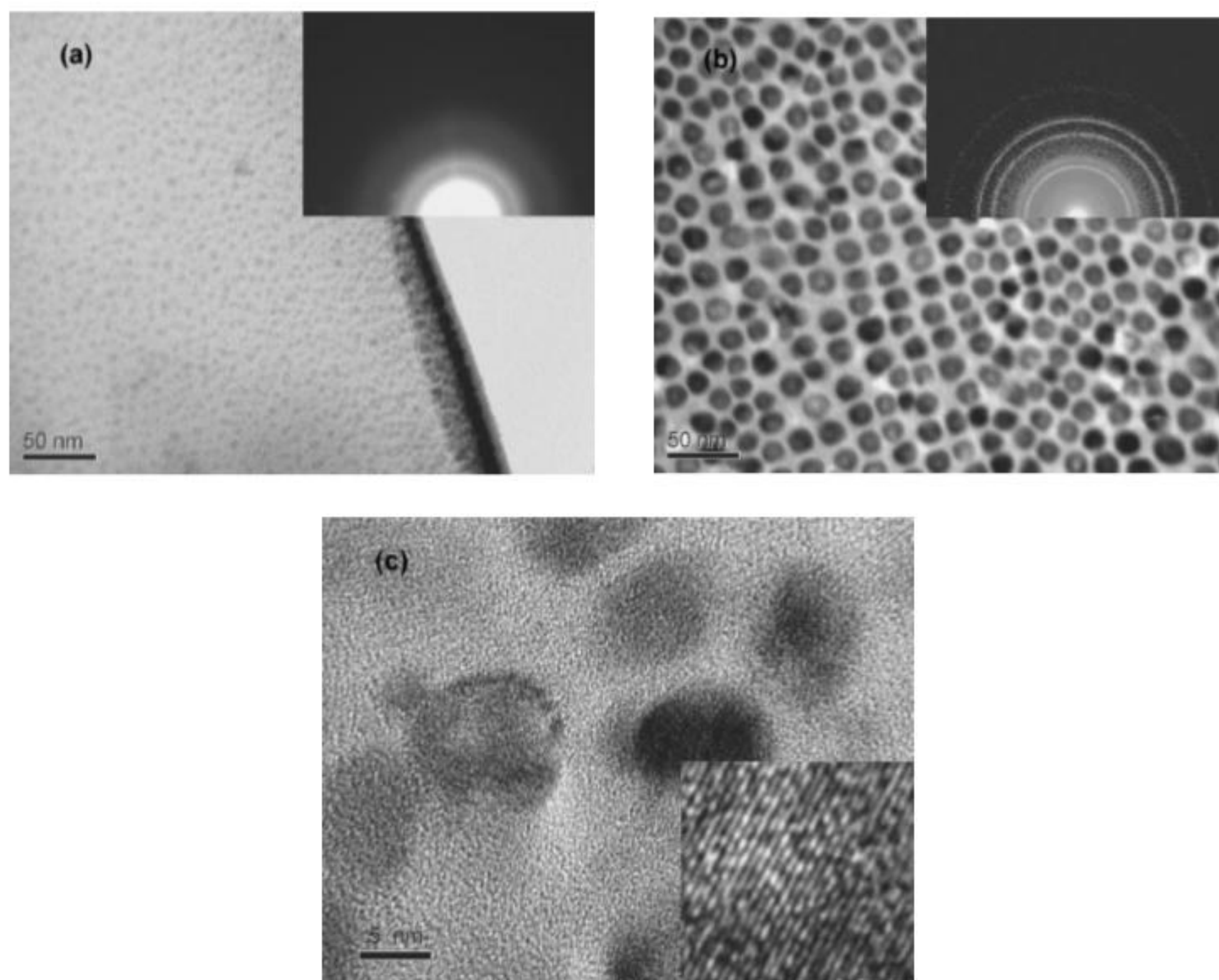

Fig. 2. (a) and (b) show TEM images of the films prepared at 50 and 100 V, respectively. The N_2 flow rate was fixed at 20 sccm and the target current was fixed at 5 A. The corresponding TED patterns are shown in the insets. (c) shows the high-resolution TEM image of the CN_x film prepared at a substrate bias of 50 V, an N_2 flow rate of 20 sccm, and a Ti target current of 5 A.

Figures 2(a) and 2(b) show TEM images and the corresponding electron diffraction patterns of samples deposited at 50 and 100 V biases, respectively. At 50 V, the film is predominantly amorphous with C, N, and Ti coexisting, as seen in the electron diffraction pattern. The film contains numerous fine faint spots with sizes of approximately 10nm, which suggests the segregation of nanometer-sized structures. When bias increases to 100V, the contrast of the grains become intense and their boundaries become clearer. The sizes of the grains are between 15 and 20nm. Five sharp diffraction circles are observed from the inset in Fig. 2(b) with d spacings of 2.07, 1.79, 1.25, 1.07, and 0.80 Å,

which cannot be matched by TiN, TiC, TiC_xN_{1-x}, Ti, or graphite. Instead, these peaks can be consistently indexed as the (210), (301), (320), (411), and (332) crystallographic places of β-C_3N_4, in accordance with the theoretical calculation and experimental results of Yu et al.[12] and Niu et al.[8] including the relative intensity of the peaks. A high-resolution TEM image of the sample deposited at 100 V bias is shown in Fig. 2(c). Nanocrystals with a size of approximately 8 nm are dispersed in an amorphous CN_x matrix. Clear crystal lattice stripes are observed with a d spacing of 1.88 Å from a Fourier transform, which do not appear in a diffraction circle due to their relatively weak intensities and correspond to the reflection of the (111) planes of β-C_3N_4. The change of the film's microstructure indicates that the formation of nanocrystals is very sensitive to substrate bias, and high-energy ion bombardment promotes the nucleation and growth of β-C_3N_4 nanocrystals.

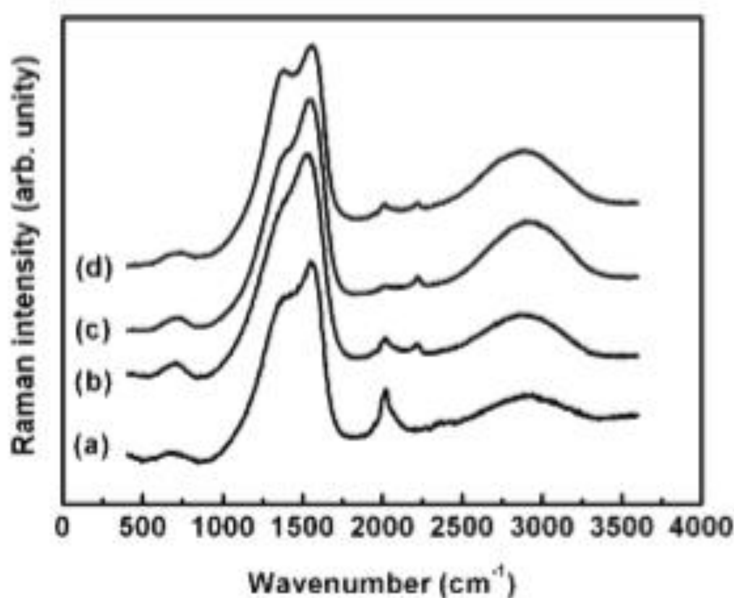

Fig. 3. Raman spectra of Ti-doped CN_x films prepared without N_2 (a) and at N_2 flow rates of 20 (b and d), and 70 sccm (c). The Ti target current for (b) is 0 A and those for (a), (c), and (d) are 5 A. The substrate bias was fixed at 50 V. The N/C ratios for (a–d) are 0, 15, 25, and 32%, respectively.

Figure 3 shows the Raman spectra of the CN_x films deposited with different deposition parameters. Six main features can be detected in these spectra and are attributed as follows: The L band, centered at approximately 700 cm^{-1}, corresponds to the out-of-plane bending mode of graphitelike domains. The D band, detected at approximately 1360 cm^{-1}, originates in the breathing modes of sp^2 atoms in aromatic six-fold rings. The band at approximately 1580 cm^{-1} is attributed to the stretching of the C=C bond, namely, the G band, which overlaps with the D band and forms the largest feature of the spectrum. The small peak at 2020 cm^{-1} is due to the existence of sp^1 C, and the peak at 2200 cm^{-1} is due to the existence of triple CN bonding. Finally, the broad band at approximately 3000 cm^{-1} is attributed to overlapped second-order D and G Raman peaks. There are no features related to Ti in any of the samples measured. There is a quite intensive sp^1 feature, which apparently is due to the absence of triple CN bonding in the samples prepared without N_2. Quantitative information is obtained from these spectra by fitting the D and G peaks to Gaussian lines. Table 1 shows the fitted peak frequencies, bandwidths, and intensity ratios of the D and G peaks. The sample deposited in pure Ar dischage exhibits a high I_D/I_G ratio as a result of the high content of Ti that diminishes the size of sp^2 C clusters. With increasing N concentration, the positions of the D and G peaks of the CN_x films are upshifted, their full widths at half maximum become narrow, and their I_D/I_G values increase. This indicates an increase in the amount of disordered C and that the concentration of sp^3 hybridized phase increases, which is consistent with the TEM result indicating the formation of β-C_3N_4 at high N concentrations.

Table 1 Wavenumber, full width at half maximum, and intensity ratio of D and G peaks obtained from fitting of Raman spectra with Gaussian functions of Ti-doped CN_x films with various N concentrations.

N / C ratio (%)	σD (cm^{-1})	ωD (cm^{-1})	σG (cm^{-1})	ωG (cm^{-1})	I_D/I_G
15	1369	368	1550	175	2.4
25	1386	355	1563	152	2.8
32	1388	349	1573	125	4.4

4. Conclusion

In summary, Ti-doped CN_x films have been deposited using an eight-target middle-frequency magnetron sputter system at various substrate biases, N_2 flow rates, and Ti target currents. Composition measurement revealed that the existence of a small amount of Ti atoms promotes the combination of N with C atoms and the nucleation of β-C_3N_4. TEM revealed a microstructure of amorphous CN_x matrix embedded with β-C_3N_4 nanocrystals with sizes of about 8 nm, which were formed by controlling the sputter power of the Ti target and N_2 flow rate.

References

[1] A. Y. Liu and M. L. Cohen: Science 245 (1989) 841.

[2] A. Y. Liu and M. L. Cohen: Phys. Rev. B 41 (1990) 10727.

[3] E. G. Wang: Adv. Mater. 11 (1999) 1129.

[4] F. Alvarez, N. M. Victoria, P. Hammer, F. L. Freire, Jr. and M. C. dos Santos: Appl. Phys. Lett. 73 (1998) 1065.

[5] L. C. Chen, T. R. Lu, C. T. Kuo, D. M. Bhusari, J. J. Wu, K. H. Chen and T. M. Chen: Appl. Phys. Lett. 72 (1998) 3449.

[6] M. Friedrich, T. Welzel, R. Rochotzki, H. Kupfer and D. R. T. Zahn: Diamond Relat. Mater. 6 (1997) 33.

[7] N. Hellgren, M. P. Johansson, E. Broitman, L. Hultman and J. E. Sundgren: Phys. Rev. B 59 (1999) 5162.

[8] C. Niu, Y. Z. Lu and C. M. Lieber: Science 261 (1993) 334. 9) Y. Aoi, K. Ono and E. Kamijo: J. Appl. Phys. 86 (1999) 2318.

[9] D. Li, X. W. Lin, S. C. Cheng, V. P. Dravid, Y. W. Chung, M. S. Wong and W. D. Sproul: Appl. Phys. Lett. 68 (1995) 1211.

[10] B. Yang, Z. H. Huang, C. S. Liu, Z. Y. Zeng, X. J. Fan and D. J. Fu: Jpn. J. Appl. Phys. 44 (2005) L1022.

[11] K. M. Yu, M. L. Cohn, E. E. Haller, W. L. Hansen, A. Y. Liu and I. C. Wu: Phys. Rev. B 49 (1994) 5034.